JOURNAL OF MATERIALS SCIENCE 37 (2002) 2909–2916

Surface repair of porous and damaged alumina bodies using carboxylate-alumoxane nanoparticles

KIMBERLY A. DEFRIEND, ANDREW R. BARRON*
Department of Chemistry, Department of Mechanical Engineering and Materials Science, and Center for Nanoscale Science and Technology, Rice University, Houston, Texas 77005, USA
E-mail: arb@rice.edu;Url:www.rice.edu/barron

Aqueous solutions of acetate-functionalized alumina nanoparticles (A-alumoxane), with an average particle size of 28 nm, have been used as alumina precursors for the surface infiltration and repair of porous and/or damaged alumina surfaces. SEM and AFM measurements indicate that treatment with a 1 wt% solution results in a reduction of surface roughness from $>0.6\ \mu$m to $\approx$100 nm for surface pores in the 100 nm to 1 μm range. The use of 6 wt% solutions gives better infiltration repair for 50 μm features, but surface cracking is observed. The surface hardness of the porous alumina substrate is increased upon infiltration. No spallation of the surface infiltration layer is observed after indentation measurements and grain dislodgment is overcome.

1. Introduction

Traditional ceramic processing involves three basic steps generally referred to as powder-processing, shape-forming, and densification, often with a final mechanical finishing step [1, 2]. Unfortunately, since a ceramic powder is mixed with various binders, solvents, and other agents to form and stabilize a solid ("green") body, and these agents are subsequently removed in gaseous form by direct evaporation and/or pyrolysis, extensive shrinkage results upon processing [3–5]. In addition, this effect is exacerbated in the case of ceramic fiber-ceramic matrix composites in which the back stress between the reinforcing phase (fiber) and the matrix results in resistance to densification, i.e., significant porosity [6]. An additional problem with ceramic composites processed through traditional routes is that the surface is rough. This occurs from the sintering step, as well as physical handling and post-sintering machining. A further problem often associated with hot pressed ceramic components is that during impact or mechanical stresses, grain dislodgment and intergranular microfracture occurs which has detrimental effects on the material's performance [7].

Possible solutions to these effects include: the use of a pre-ceramic polymer as the binder to minimize porosity [8], post-process micro-machining and post-process surface infiltration of the porous ceramic [9–11]. Sintering of an infiltrated pre-ceramic material will cause the formation of a second ceramic material within the original substrate. Clearly, this can be of the same crystalline phase or designed to enhance the reinforcing phase (i.e., fiber) and the matrix interactions [12]. Infiltration of porous ceramics by metals has previously been used to strengthen bulk ceramic bodies [13, 14].

It is desirable that any infiltration and/or surface repair medium should have a high ceramic yield but should also have a small particle size such that defects on the sub micron scale can be treated. Although sol-gel methods could possibly be used for this application, high ceramic yields are traditionally associated with large particle size. Additionally, it would be advantageous for a surface infiltration process to provide a planarization function [15]. Since, such a process will undoubtedly result in a new surface layer it is necessary that the infiltrating material form a graded interface [16, 17] with the bulk material to minimize spallation and failure. Finally, it would be desirable for all treatments to be carried out in water with minimal use of volatile organic chemicals (VOCs). In this regard, we have developed an environmentally benign, versatile method of solubilizing aluminum oxide nanoparticles by reacting boehmite, $[Al(O)(OH)]_n$, with carboxylic acids, (HO_2CR), in aqueous conditions [8]. The resulting materials are known as carboxylate-alumoxanes. Photon correlation spectrocsopy (PCS) measurements indicate that the alumoxanes are chemically functionalized nanoparticles and may be selectively prepared with a particle size of 5–150 nm depending on the identity of the organic substituents [8] and the processing conditions [18]. Unlike traditional sol-gels, the alumoxane nanoparticles have a high ceramic yield (>70%)

*Author to whom all correspondence should be addressed.

and therefore show low shrinkage upon thermolysis [8]. Furthermore, although pyrolysis of the alumoxanes produces alumina, the alumoxane nanoparticles undergo a unique metal exchange reaction that allows for the convenient formation of phase pure aluminates, e.g., $Y_3Al_5O_{12}$ (YAG) [19], $CaAl_{12}O_{19}$ (hibonite) [20], $MgAl_2O_4$ [21]. Thus, they may be used to prepare hetero-phase composites [21].

Herein we report our initial studies into the surface repair of porous and damaged alumina bodies using the carboxylate-alumoxane nanoparticles. The present study is only concerned with surface repair, and

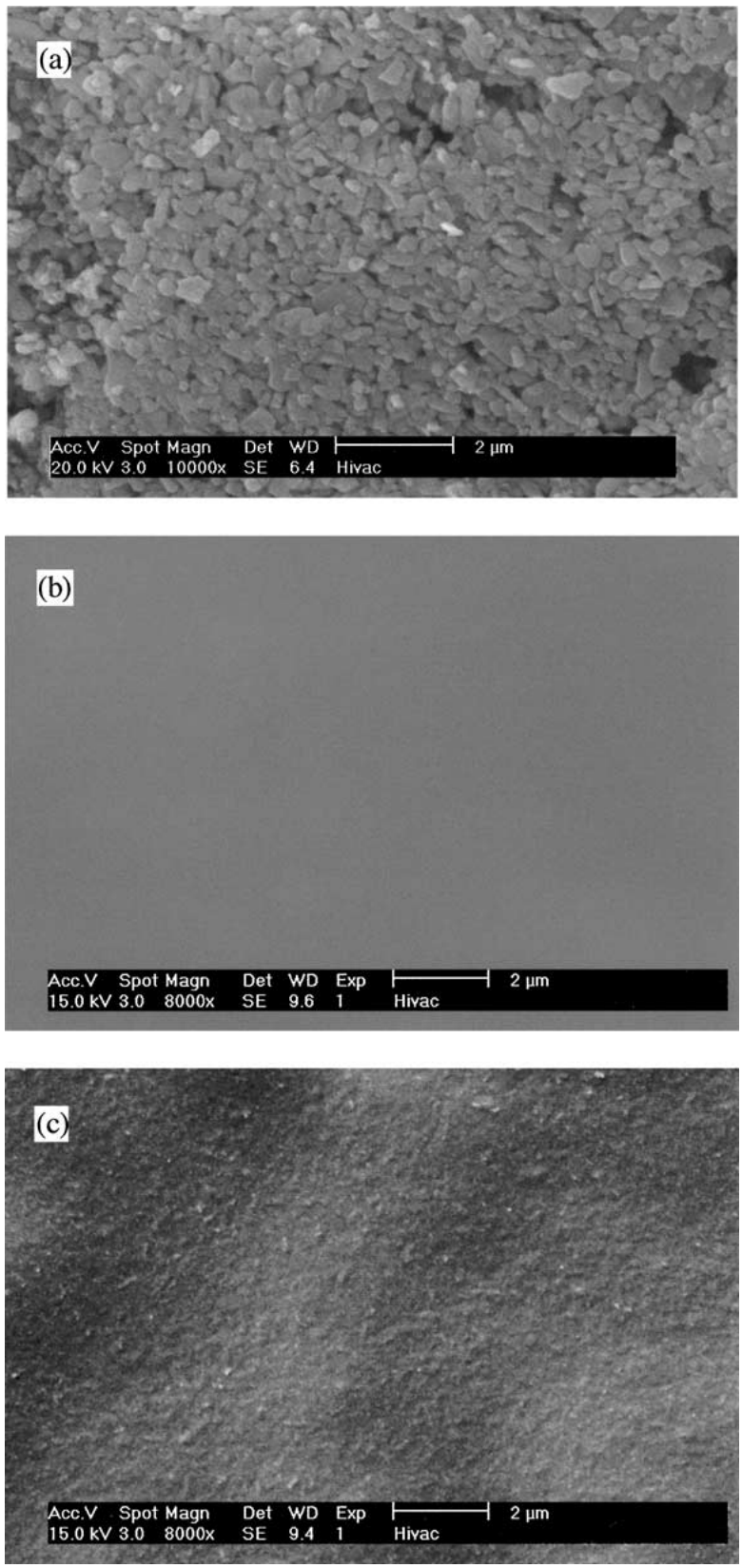

Figure 1 SEM image of the top surface of a commercial α-alumina support (a) before treatment, (b) after treatment with 1% solution of A-alumoxane nanoparticles and (c) after sintering to 1000°C.

our studies on bulk body infiltration will be reported elsewhere.

2. Experimental procedure

2.1. General

Acetate-alumoxane (A-alumoxane) nanoparticles were prepared by the reaction of acetic acid (HO_2CCH_3) and boehmite, using previously published methods [8]. Standard aqueous solutions of 1 wt% and 6 wt% A-alumoxane were prepared by stirring A-alumoxane in DI water until completely dissolved. The standard solutions may be stored indefinitely before use without precipitation or gelation. Circular α-alumina supports (48 mm diameter, 2 mm thickness) were obtained from the Refractron Technologies Corp. (Newark, NY). Supports were washed with acetone and heated to 600°C before use to remove surface grease.

Scanning electron microscopy (SEM) studies used to determined the surface roughness, and the uniformity of the infiltration, were performed on a Phillips XL-30 ESEM at 15 kV. The samples were mounted on carbon tape and sputter coated with gold. Cross-sections of the infiltrated substrates were performed to address the extent of filled in scratches. Atomic force microscopy (AFM) measurements were made on a Nanoscope IIIa Scanning Probe Microscopic Controller (Digital Instruments). Probes were FESP supplied by Digital Instruments and were used in the tapping mode. The scan rate was 1 Hz, and the number of samples taken on the fast scan axis was 512 per line. Roughness and cross-section analysis were determined by the accompanying Nanoscope IIIa software. Microindention testing was performed on a Micromet microhardness tester. Load weights varied with the sample. The hardness was determined by inserting the load weight and the area of indention into the Vicker's equation: $H_v = 1.85444(P/d^2)$ where P is the load in kg and d^2 is the area of indention in mm^2. A minimum of six measurements was made on each sample. Contact angle measurements were performed in a clean air hood, at a humidity of 48–50% and an ambient room temperature of 22–24°C.

2.2. Surface infiltration of alumina substrates

A Refractron^{TM} α-alumina support was brought into contact with an A-alumoxane solution (1 or 6 wt%) so that only the surface touched the solution for approximately 2–5 seconds. The support was then shaken to remove any excess solution, and dried at room temperature for 2 hours. The coated support was heated to 600°C over four hours, held for 3 hours, and then heated to 1000°C for three hours. Multiple coatings were obtained by treating a previously coated support (1 wt% A-alumoxane) fired to 1000°C, with a 1 wt% aqueous solution of A-alumoxane followed by firing, unless otherwise noted, to 1000°C. Where indicated, multiple dip-fire procedures were carried out. The surface of an Al_2O_3 Refractron^{TM} disc was scratched using a sharp glass tip to damage the surface. The surface was then subjected to high-pressure air to remove any particulate matter present. The damaged surface was treated in the manner described above.

3. Results and discussion

For our initial studies into the suitability of alumoxane nanoparticles as surface repair agents we chose to use a well characterizable alumina substrate with consistent surface porosity and morphology from sample-to-sample. In this regard, commercially available α-alumina porous disks were used. From the SEM images of the surface of the Refractron^{TM} α-alumina substrate (Fig. 1a), they are composed of alumina particles sintered together with particle sizes ranging from 0.05–1 μm. Many surface defects are observed, including a significant number of void spaces on the top surface of the substrate. AFM analysis shows an average roughness of >0.6 μm over a 4 μm scan length (Fig. 2a). From AFM measurements the pores appear to range from 100 nm to 1 μm in cross section. Nitrogen absorption confirms the presence of a broad distribution of pores with a maximum pore size over 180 nm [22]. Initially 1 wt% solutions of A-alumoxane were employed based upon prior results with coating sapphire, carbon, and SiC fibers [23, 24] in which highly uniform coatings were obtained with minimal surface cracking.

The choice of the acetate substituted alumoxane (A-alumoxane) was dictated by the following factors: (1) a

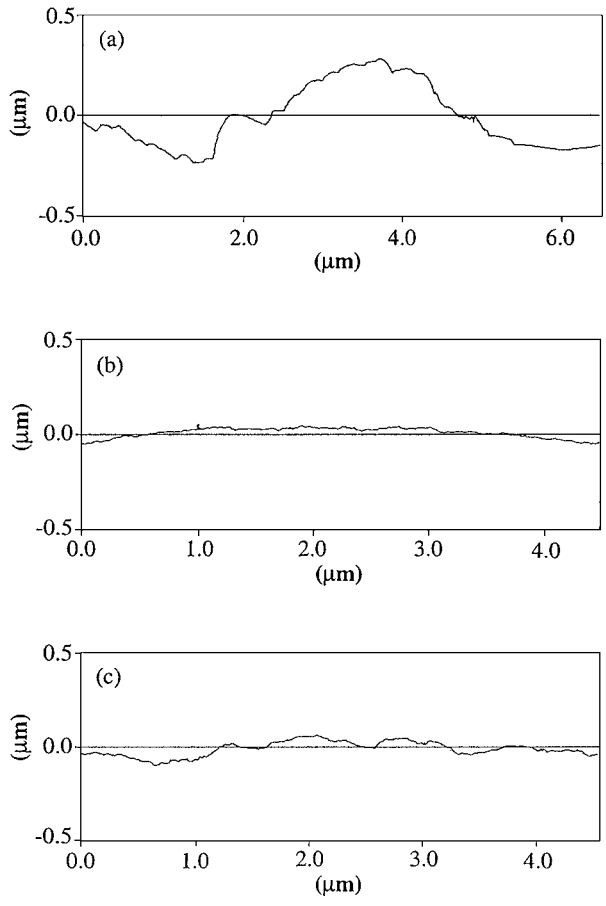

Figure 2 The AFM of the top surface of (a) a commercial α-alumina support showing the typical surface roughness, (b) after treatment with 1% solution of A-alumoxane nanoparticles and (c) after sintering to 1000°C.

high ceramic yield (ca. 76%) minimizes shrinkage upon thermolysis; (2) an average particle size at neutral pH of 28 nm allows for infiltration into the pores of the chosen substrate [18]; (3) a high solubility in water of 0.20 g mL^{-1} allows for aqueous processing [8].

On the basis of SEM (Fig. 1b) and AFM (Fig. 2b) measurements the surface roughness decreases from $>0.6\ \mu$m of the untreated substrate to ca. 100 nm after air drying the alumoxane treated substrate. After firing the samples to 1000°C (Fig. 1c), the surface roughness

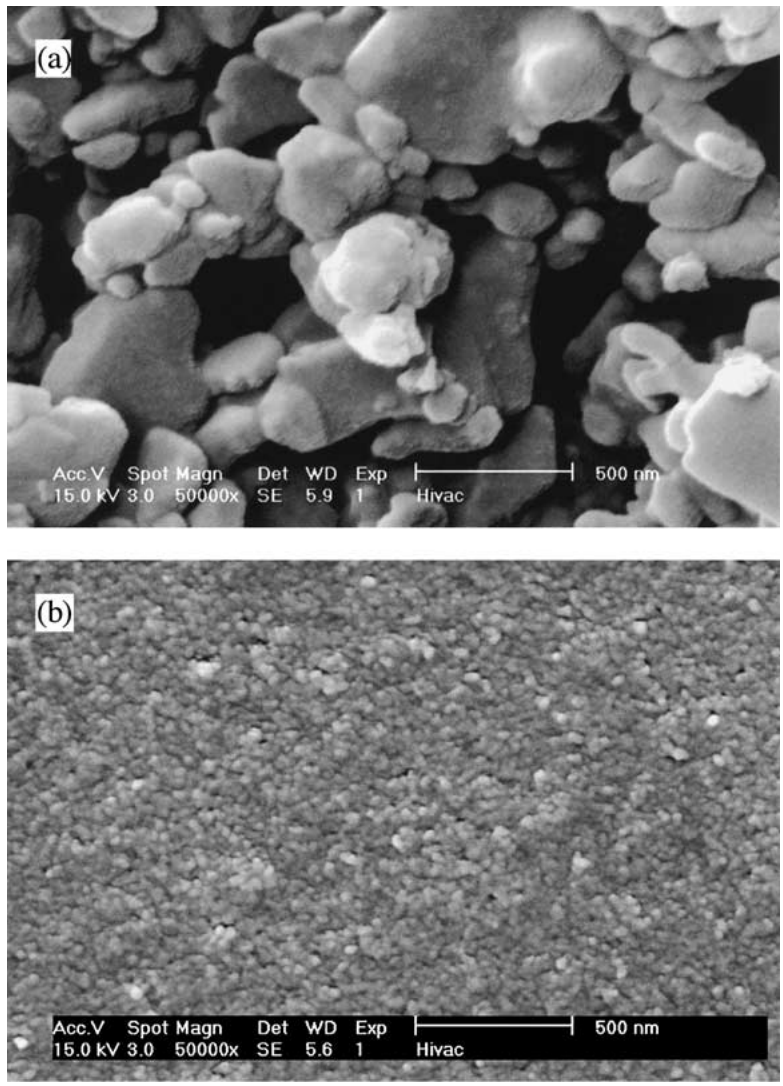

Figure 3 SEM images (× 50,000) of the top surface of a commercial α-alumina support (a) before treatment and (b) after infiltration and sintering to 1000°C, showing the full infiltration of voids and planaraization of the surface.

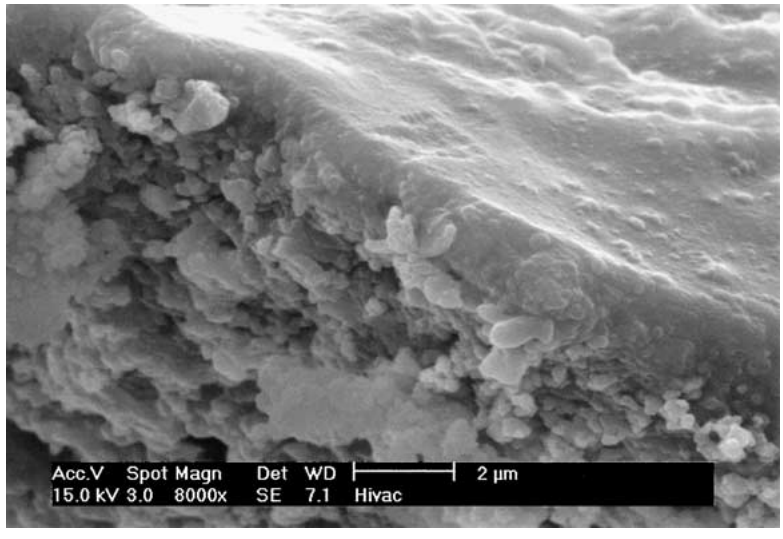

Figure 4 SEM image of a cross section of a treated commercial α-alumina support.

increases slightly to ca. 200 nm (Fig. 2c), presumably due to the shrinkage of the infiltrated material upon pyrolysis. The lowest roughness obtained with 1 wt% solutions is ca. 100 nm after two dip-and-fire sequences. No further improvement is observed with further dip and fire sequences.

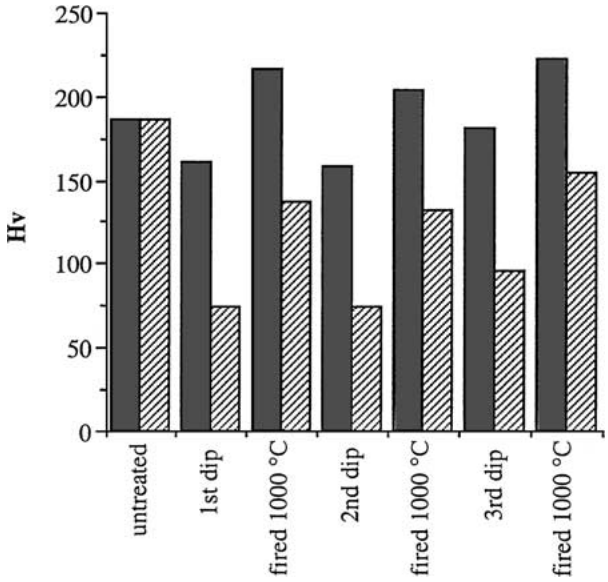

Figure 5 A bar graph showing the Vickers hardness of α-alumina support before and after each dip treatment with 1 wt% (■) and 6 wt% (▨) alumoxane solution and the subsequent thermolysis to 1000°C.

A comparison of the surface pre- and post-infiltration is shown in Fig. 3. It may be clearly seen that full infiltration of voids has been accomplished and planarization of the surface has resulted. The infiltrated material has a microstructure consisting of highly uniform grains ca. 25 nm in size, consistent with the uniform nanoparticulate nature of the A-alumoxane. Based upon separate sintering studies, firing the A-alumoxane to 1000°C results in a mixed phase material consisting of predominantly θ-Al_2O_3 (JCPDS # 35-0121) and minor component of α-Al_2O_3 (JCPDS # 42-1468) [25].

SEM images of a cleaved cross section (e.g., Fig. 4) indicate that the infiltration is limited to a surface layer of between 1–2 μm in depth. A decrease in infiltration is observed with depth from the surface of the substrate. The surface of the substrate is fully infiltrated, but, below ca. 2 μm, the bulk of the substrate is unaffected. The surface infiltration process results in a graded interface, shown in Fig. 4.

The hardness of the untreated substrate was determined to be 2.13 ± 0.03 G Nm^{-2}. This is within the range expected from the temperature at which the substrates are sintered during fabrication (1000°C). As expected, the hardness of the surface decreases after dip-coating with the alumoxane solution

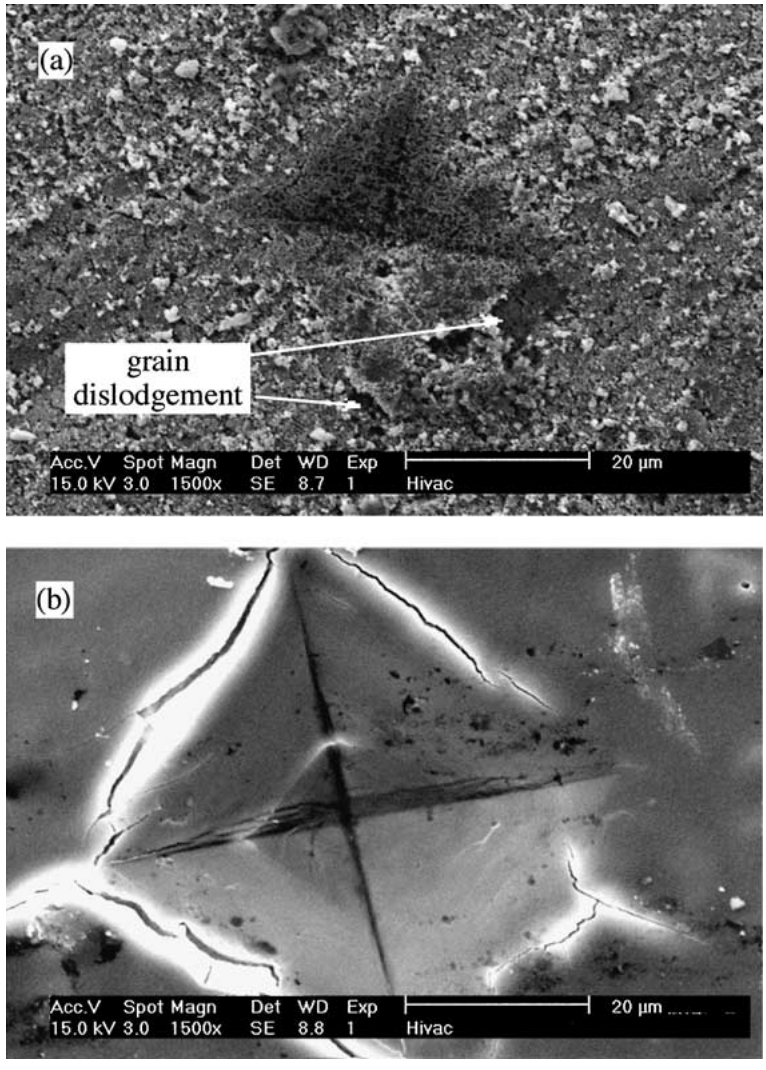

Figure 6 SEM image of the surface of (a) an α-alumina support and (b) a A-alumoxane treated support after micro-indention testing.

(1.5 ± 0.2 G Nm^{-2}), due to the relatively soft nature of the alumoxane nanoparticles (ca. 0.88 G Nm^{-2} for a film of A-alumoxane formed by evaporation of an aqueous solution [8]). Upon thermolysis, the hardness increases to 2.2 ± 0.6 G Nm^{-2}. Each dip coat treatment with the alumoxane solution results in an appropriate decrease in hardness, which then increases with the firing step, see Fig. 5. The microhardness is not expected to rise significantly due to the small area of measurement, but the surface density is expected to rise due to the infilling of the surface pores. As expected, thermolysis of the alumoxane nanoparticle infiltrated substrate

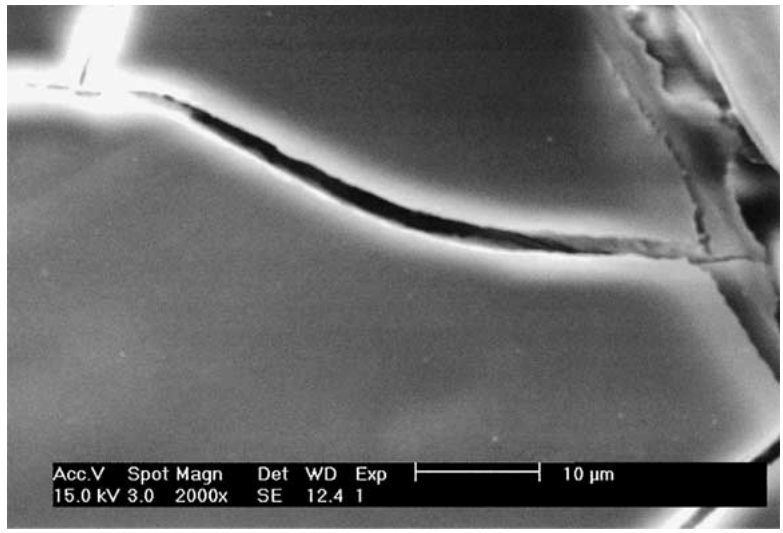

Figure 7 SEM image of the surface of an α-alumina support after dip treatments with an aqueous 6 wt% solution of A-alumoxane, showing the presence of extensive cracking in some areas.

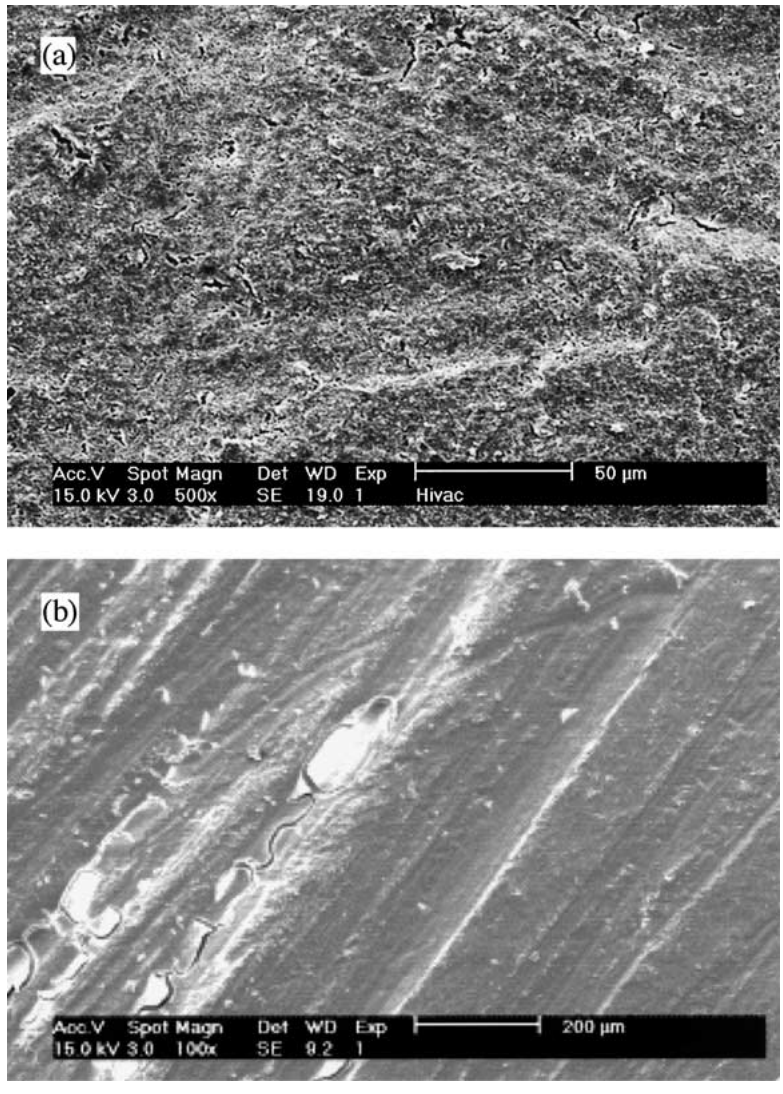

Figure 8 SEM image of the surface of an intentionally damaged α-alumina support after treatment with an aqueous 6 wt% solution of A-alumoxane.

to 1400°C for 12 hours results in a further increase in hardness (10.5 ± 0.5 G Nm^{-2}). A similar, but more variable, result is obtained by sintering the untreated substrate under the same conditions (12 ± 3 G Nm^{-2}). Interestingly, infiltration of a previously sintered substrate results in a significant further improvement in hardness ($>15 \pm 4$ G Nm^{-2}).

The α-alumina substrates are coarse grained, and as such, grain dislodgment and intergranular microfracture occur during impact or mechanical stresses. For example, significant grain dislodgment is seen to occur during hardness measurements in which stress is applied to the surface (Fig. 6a). In contrast, when the finely granular ceramic formed from the A-alumoxane is infiltrated into the surface of the ceramic body, the small particles (Fig. 3b) act as a binder towards the large grains of the substrate (i.e., Fig. 3a), weaving around and between the grains. Therefore, when a force is applied to the ceramic surface, the smaller particle size ceramic prohibits grain dislodgment, by decreasing surface porosity and increasing the surface area, through infiltration between the coarse grains of the surface. Although cracking occurs after micro-indention testing (Fig. 6b) there appears to be no grain dislodgment. Furthermore, no spallation is observed, confirming that the treatment results in infiltration rather than a coating.

Substrates treated using a 6 wt% solution of the alumoxane nanoparticles were observed to have a high fraction of defects (cracks, agglomerates, etc.), presumably due to non-uniform drying (e.g., Fig. 7). This is continued through the sintering step as may be seen in the SEM images. A second problem with 6 wt% solution is that hardness is lower after the first dip and fire treatment and only returns to the original level after multiple dip and fire cycles (Fig. 5). These effects suggest that the 6 wt% solution primarily results in coating rather than infiltration of the substrate's surface layer. Thus, it appears that the 1 wt% solution of A-alumoxane nanoparticles is most suited for the surface repair of <10 μm porosity and/or damage.

Despite the microscopic roughness, the Refractron^{TM} α-alumina substrates have only small macroscopic defects. To determine the suitability of this method for macroscopic damage, as would be associated with machining, 50 μm wide, 2 μm deep scratches were made into the surface. Infiltration with 1 wt% solutions of alumoxane nanoparticles did not significantly effect these large features, except after multiple dip and fire sequences. In contrast, the 6 wt% solutions give better infiltration (coating) of damage in the 100–150 μm range. AFM measurements show microscopic roughness isn't any different, but macroscopic damage is improved giving a slight shadow (Fig. 8a). In addition, SEM images show that as damage features decrease some cracking of "in-fill" area is observed if drying is too fast (e.g., Fig. 8b).

Thus, there appears to be a trade-off with the use of various wt% solutions of the alumoxane nanoparticles between macroscopic damage repair and microscopic surface infiltration. The solution to this dichotomy is to use of 6 wt% solution with a subsequent 1 wt% treatment to repair 15–20 μm cracks. We have previously shown that cracks that occur in rapid drying of SiC and sapphire fibers can be repaired in this manner [23, 24].

4. Conclusions

The carboxylate-alumoxane nanoparticles are a novel, environmentally benign alumina precursor for the surface repair of porous and/or damaged ceramic surfaces. Initial studies indicate that lower concentration aqueous solutions (1 wt%) are more efficient at infiltration of <10 μm features. Although higher concentration solutions allow for repair of large features, significant cracking can occur due to rapid solvent evaporation (that must be subsequently treated). Surface roughness can be improved with up to two or three treatments, but no further improvement is seen with subsequent dip and fire cycles. The alumoxane nanoparticle treatment results in the infiltration of the surface and a graded interface with the bulk porous substrate, rather than a coating.

The ability to use the alumoxane nanoparticles to infill <10 μm features suggests that this methodology may also be used for planarization or isolation layers in electronic devices. It should be noted that while the dielectric constant (ε) of the alumoxane is 2.5 (@ 10^3 Hz), the alumina formed upon thermolysis has the expected value (4.5–8.4 @ 10^6 Hz).

The present study is concerned with surface infiltration, as opposed to full infiltration of the ceramic body. Given the ability of the alumoxane nanoparticles to be doped with a variety of metals [15, 16], and their subsequent mild conversion to phase pure aluminates, our future work will be aimed at the full infiltration of a porous alumina substrate with heterometallic alumoxane nanoparticles (e.g., yttrium doped alumoxane) such that upon thermolysis the resulting material will be an alumina/aluminate composite (e.g., Al_2O_3/YAG and Al_2O_3/$LaAlO_3$). These results will be presented elsewhere [21].

Acknowledgment

Financial support for this work was provided by the National Aeronautics and Space Administration.

References

1. W. D. KINGERY, H. K. BOWEN and D. R. UHLMANN, "Introduction to Ceramics," 2nd ed. (Wiley, New York, 1976) ch. 1.
2. D. W. RICHERSON, "Modern Ceramic Engineering" (Marcel Dekker, New York, 1992) p. 373.
3. J. A. MANGELS and G. L. MESSING (eds.), "Advances in Ceramics," Vol. 9 (American Ceramic Society, Westville, OH, 1984).
4. D. VOLTZKE and H.-P. ABICHT, *J. Mater. Sci. Lett.* **19** (2000) 1951.
5. L.-S. CHEN, S.-L. FU and W.-K. HUANG, *Jpn. J. Appl. Phys., Part 1* **39** (2000) 5209.
6. H. F. LOPEZ and W. PHOOMIPHAKDEEPHAN, *J. Mater. Sci.* **35** (2000) 5995.
7. H. H. K. XU and S. JAHANMIR, *ibid.* **30** (1995) 2235.
8. R. L. CALLENDER, C. J. HARLAN, N. M. SHAPIRO, C. D. JONES, D. L. CALLAHAN, M. R. WIESNER, D. B. MACQUEEN, R. COOK and A. R. BARRON, *Chem. Mater.* **9** (1997) 2421.
9. D. R. GABE, "Coatings for Protection" (Institution of Production Engineers, London, 1983).

10. I. LEE, *J. Mater. Sci. Lett.* **20** (2001) 223.
11. I. B. INWANG, I. J. MCCOLM and A. WRONSKI, *J. Mater. Sci.* **36** (2001) 1823.
12. R. L. CALLENDER and A. R. BARRON, *J. Mater. Res.* **15** (2000) 2228.
13. A. R. KENNEDY, J. D. WOOD and B. M. WEAGER, *J. Mater. Sci.* **35** (2000) 2909.
14. C. KAWAI and J.-J. PARK, *J. Mater. Sci. Lett.* **20** (2001) 385.
15. A. C. ADAMS and C. D. CAPIO, *J. Electrochem. Soc.* **128** (1981) 2630.
16. P. RENDTEL, F. WAGNER, R. JANSSEN and N. CLAUSSEN, *Mater. Sci. Forum* **308–311** (1999) 181.
17. A. N. MACINNES, A. R. BARRON, R. S. SOMAN and T. R. GILBERT, *J. Amer. Ceram. Soc.* **73** (1990) 3696.
18. C. T. VOGELSON and A. R. BARRON, *J. Non-Cryst. Solids*, in press.
19. C. J. HARLAN, A. KAREIVA, D. B. MACQUEEN, R. COOK and A. R. BARRON, *Adv. Mater.* **9** (1997) 68.
20. R. L. CALLENDER and A. R. BARRON, *J. Amer. Ceram. Soc.* **83** (2000) 1777.
21. K. A. DEFRIEND and A. R. BARRON, submitted.
22. C. D. JONES, M. FIDALGO, M. R. WIESNER and A. R. BARRON, *J. Membrane Sci.* **193** (2001) 175.
23. R. L. CALLENDER and A. R. BARRON, *J. Mater. Res.* **15** (2000) 2228.
24. *Idem.*, *J. Mater. Sci.* **36** (2001) 4977.
25. C. D. JONES, D. A. BAILEY, M. R. WIESNER and A. R. BARRON, in 9th CIMTEC-World Ceramics Congress, Ceramics Getting into the 2000—Part D (1999) p. 413.

Received 24 July 2001
and accepted 12 March 2002